

Regular transport dynamics produce chaotic travel times

Jorge Villalobos,^{1,2,*} Víctor Muñoz,³ José Rogan,^{3,4} Roberto Zarama,^{2,5} Neil F. Johnson,^{2,6}
Benjamín Toledo,³ and Juan Alejandro Valdivia^{2,3,4}

¹*Facultad de Ciencias Naturales y Matemáticas, Universidad de Ibagué, Ibagué, Colombia*

²*CEIBA Complejidad, Bogotá, Colombia*

³*Departamento de Física, Facultad de Ciencias, Universidad de Chile, Santiago, Chile*

⁴*CE DENNA, Santiago, Chile*

⁵*Departamento de Ingeniería Industrial, Universidad de los Andes, Bogotá, Colombia*

⁶*Physics Department, University of Miami, Florida 33126, USA*

(Received 23 July 2013; revised manuscript received 2 September 2013; published 27 June 2014)

In the hope of making passenger travel times shorter and more reliable, many cities are introducing dedicated bus lanes (e.g., Bogota, London, Miami). Here we show that chaotic travel times are actually a natural consequence of individual bus function, and hence of public transport systems more generally, i.e., chaotic dynamics emerge even when the route is empty and straight, stops and lights are equidistant and regular, and loading times are negligible. More generally, our findings provide a novel example of chaotic dynamics emerging from a single object following Newton's laws of motion in a regularized one-dimensional system.

DOI: [10.1103/PhysRevE.89.062922](https://doi.org/10.1103/PhysRevE.89.062922)

PACS number(s): 05.45.-a, 89.40.Bb, 45.70.Vn, 89.75.Da

As well as representing a major global socioeconomic challenge in the 21st century, the problem of city traffic has developed into an active area of theoretical research [1–12], in particular among physicists. The underlying assumption is that by understanding the collective dynamics of vehicles in realistic road layouts, insights can be gleaned which will translate into practical solutions. Such insights may also have an application to other areas, for example, for understanding the intracellular transport of kinesin motors on microtubules [13].

Similar to kinesin motors, whose function is to carry a molecular load, buses serve the function of regularly transporting groups of people according to some externally determined scheduling criteria. Since they feature so heavily in everyday urban traffic, buses are also the target of frequent complaints concerning erratic waiting and travel times. Studies exist of school buses [14], the effect of bus stops on city traffic [15, 16], bus-flow optimization and vehicle location techniques [17–19], priority lane usage [20–25], and bus priority methods for traffic light control [26]. Moreover the notoriety of buses for arriving in threes, otherwise known as bus bunching or platooning [27], has been explained in terms of a snowball collective effect whereby a particular bus suffers a momentary delay for some external reason, introducing a bottleneck behind which other buses bunch. The focus in such studies is implicitly towards the collective behavior of traffic, in particular the effects of multivehicular interactions.

Here we strip down the analysis of bus travel to a bare minimum: A single bus traveling along an empty, straight road with equidistant, regular stops and traffic lights showing no phase lags. Even in the absence of unexpected external delays due to loading times at bus stops or interactions with other vehicles, we find that a remarkably complex dynamics emerges. We conclude that chaotic passenger travel and waiting times are an inherent feature of public transport

systems, emerging from the need for regular stops combined with background flow control (i.e., periodic traffic lights).

Our model employs Newton's laws of motion in continuous time and space, thereby allowing us to include realistic effects such as acceleration after stopping, deceleration ahead of a red light, and a finite speed limit. Moreover, the motion during each portion of the journey (see Fig. 1) is determined analytically as shown in the Appendix. The fact that the complexity of the emerging dynamics is so unexpected may explain why this simple one-body, one-dimensional system has received such little attention to date [6]. Each of its rules and parameters can be generalized without affecting the main results, however, for simplicity we take the separation between light n and $n + 1$ as L for all n , and assume the n th light is green at time t if $\sin \omega t \geq 0$ and is red otherwise. The parameter ω is the frequency of the traffic lights, which for simplicity we assume the same for all traffic lights. To avoid introducing spurious incommensurability effects, we set the bus stop midway between consecutive lights, at $l = L/2$. We assume that the bus stops at this bus stop for a time γ , before it starts to move again. Under optimal conditions the bus will stop for a very short time, namely $\gamma = 0$, however, in many situations we will have $\gamma > 0$ as shown in Region 4 of Fig. 1. The road speed limit is v_{\max} . In an attempt to reach that velocity, the bus is free to accelerate at a fixed rate a_+ , which is predetermined by its motor capacity. Likewise, it can decelerate at a fixed rate a_- . The dynamics described above corresponds to a nontrivial modification of the car model presented in Ref. [6], and analyzed in detail in Refs. [1, 7, 8], which is adapted for buses as it introduces the intricacies of the bus stops into the dynamics. Even when the bus spends a negligible amount of time at the bus stop (i.e., $\gamma = 0$), the bus dynamics is different from the one defined in the car model, as the bus must brake with a_- from the cruising speed v_{\max} for a finite time and distance to stop at the bus stop, for a time γ , and then accelerate from rest at the bus stop with a_+ to reach the cruising speed v_{\max} for a finite time and distance. Although at first sight one may conclude that the dynamics is exactly the same as that of a car with a reduced speed between lights, this is not the case since

*jorge.villalobos@unibague.edu.co

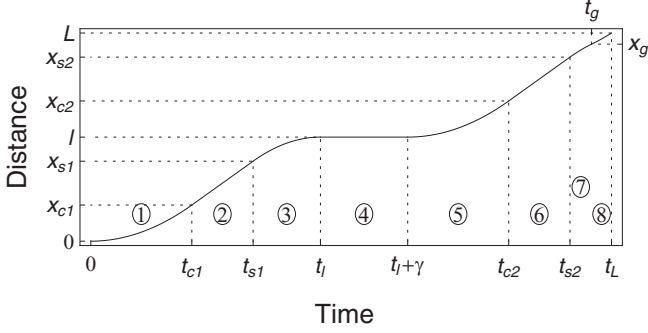


FIG. 1. Distance x traveled by a bus between two consecutive traffic lights at $x = 0$ and $x = L$, with a compulsory passenger stop at $x = l$, as a function of time t . Case shown corresponds to bus starting from a red light ($x = 0$, $t = 0$), while the upcoming light is red when $x = x_{s2}$, but changes to green before the bus reaches $x = L$.

a finite loading time ($\gamma \neq 0$) provides a nontrivial interplay between the time scales of the traffic light period and the travel time of the buses. Hence, these two features are finally responsible for the nontrivial behavior that occurs in this model (see the Appendix). The distance L between traffic lights is restricted so that the bus has enough time and distance to brake from v_{\max} and accelerate to v_{\max} after the bus stop within the traffic lights. We will see below that this additional bus-stop dynamics, compounds in a natural manner the complexity of the vehicle motion, especially when the bus-stop time $\gamma \neq 0$. This nontrivial behavior is only possible under the assumption of finite accelerating and braking capacities, and it disappears when these parameters are taken to infinity, as it happens, for example, in the popular cellular automaton model proposed by the authors of Ref. [28] (see the analysis below). Appendix A details how the motion is iterated between the n th and $(n + 1)$ th traffic light. We choose typical traffic parameters, which happen to closely match the Transmilenio bus system in Bogota, Colombia: $L = 400$ m, $a_+ = 1$ m/s², $v_{\max} = 60$ km/h, and $a_- = -5.5$ m/s².

Figure 1 illustrates the dynamics between two consecutive lights, in the case where the bus was initially stopped at a red light. The general case is given in the Appendix. In region 1, the bus accelerates until it reaches v_{\max} , i.e., at $x_{c1} = v_{\max}^2/2a_+$ following Newton's laws of motion. It continues at v_{\max} in region 2. It starts to decelerate at $x_{s1} = l - v_{\max}^2/2a_-$ (region 3) so that it stops at the upcoming bus stop ($x = l$), where it sits for time γ (region 4). It then accelerates (region 5), reaching v_{\max} at $x_{c2} = l + v_{\max}^2/2a_+$ (region 6). If the upcoming light is green at x_{s2} , it continues with v_{\max} and crosses the light. If it is red, the bus starts to decelerate when $x_{s2} = L - v_{\max}^2/2a_-$ (region 7). If it turns green after deceleration starts, the bus accelerates again (region 8). We take $l > (v_{\max}^2/2a_+ + v_{\max}^2/2a_-)$ so that regions 2 and 6 are guaranteed to exist. We also take $\omega/2\pi \leq \min(a_+, a_-)/v_{\max}$ so that the light does not change more than once while the bus is in regions 7 and 8. Defining the cruising time $T_c = L/v_{\max}$, it is convenient to write the normalized accelerations $A_{\pm} = a_{\pm}L/v_{\max}^2$, and the normalized waiting time $\Gamma = \gamma/T_c$. With these definitions, the minimum time t_{\min} between two consecutive lights when $\gamma = 0$ is

$$\frac{t_{\min}}{T_c} = 1 + \frac{1}{2} \left(\frac{1}{A_+} + \frac{1}{A_-} \right). \quad (1)$$

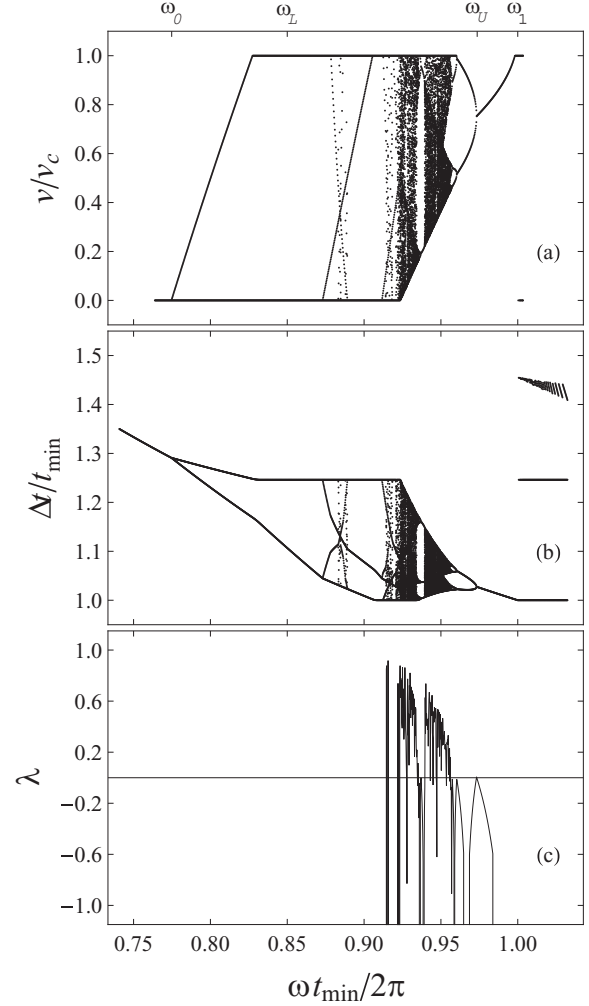


FIG. 2. Bifurcation diagrams as a function of $\omega t_{\min}/2\pi$ for (a) speed at the n th light; (b) travel time between consecutive lights; and (c) the Lyapunov exponent. Here the bus-stop loading time is $\gamma = 0$. For a given value of $\omega t_{\min}/2\pi$ the first 1000 points of the trajectory are erased as a transient, and we plot only the following 1000 values.

Initially we assume that the bus stops at the bus stop for an extremely short time γ (i.e., $\gamma = 0$), however, we will generalize this later. Figure 2(a) shows the bifurcation diagrams which emerge as a function of $\omega t_{\min}/(2\pi)$ for (a) the normalized speed v/v_{\max} as the bus passes the n th light. Figure 2(b) demonstrates the travel time between successive traffic lights $\Delta t/t_{\min}$ and Fig. 2(c) shows the Lyapunov exponent. Figure 2 represents the steady-state dynamics of the system. Even though the bus-stop loading time is $\gamma = 0$, complex dynamics including chaos emerges for $\omega_L < \omega < \omega_U$. The parameter ω_U is the first frequency below ω_1 where a period-doubling bifurcation occurs, while ω_L indicates the intersection between the lower branch of the period two orbit and the zero velocity state. Full details of the phase space and trajectories will be presented elsewhere. For $\omega = \omega_1 \equiv 2\pi/t_{\min}$, the bus is in resonance with the traffic light, crossing it at a speed v_{\max} without stopping. For $\omega \gtrsim \omega_1$, the travel time grows because the vehicle spends a larger fraction of its

time waiting for red lights to change. The regime $\omega \lesssim \omega_1$ is much richer: The bus has to decelerate, at least temporarily, before every light and chaos emerges as the light frequency is reduced. We can show that the *chaotic region* is indeed chaotic by computing the numerical maximum Lyapunov exponent as was done by the authors of Refs. [6,8] for a single car model. We evolve $(v_0, t_0) = (0, 0)$ for 10^4 iterations to make sure we are at the attractor, and then we follow the actual trajectory (x_n, t_n) and a different perturbed trajectory $(\tilde{x}_n, \tilde{t}_n)$, in which the initial normalized time was perturbed by 10^{-5} for 20 additional steps.

As $\omega \rightarrow \omega_0$, the bus stops completely at every traffic light and hence spends increasing time waiting for the green light. The parameters ω_0 , ω_L , ω_U , and ω_1 can all be calculated analytically as functions of a_+ , a_- , γ , v_c , and T_c . For example, in terms of the normalized quantities, we have

$$\begin{aligned} \frac{\omega_U T_c}{2\pi} &= \frac{2A_- A_+ (A_- + A_+)}{A_-^2 (2A_+ (\Gamma + 1) + 1) + 2A_+ A_- (A_+ (\Gamma + 1) + 1) + 5A_+^2}, \\ \frac{\omega_L T_c}{2\pi} &= \frac{A_- A_+ (A_- + A_+)}{A_-^2 (A_+ (\Gamma + 1) + 1) + A_+^2 A_- (\Gamma + 1) + 3A_+^2}. \end{aligned} \quad (3)$$

The resonant frequency ω_1 can be derived from Eq. (1), as

$$\frac{\omega_1 T_c}{2\pi} = \frac{1}{\frac{t_{\min}}{T_c} + \Gamma}. \quad (4)$$

These expressions have been used to label the relevant points in Fig. 2. It is interesting to note that when the braking capacity tends towards infinity, namely $A_- \rightarrow \infty$, we have

$$\begin{aligned} \frac{\omega_1 T_c}{2\pi} &= \frac{2A_+}{2A_+ (\Gamma + 1) + 1}, \\ \frac{\omega_0 T_c}{2\pi} = \frac{\omega_U T_c}{2\pi} = \frac{\omega_L T_c}{2\pi} &= \frac{A_+}{A_+ (\Gamma + 1) + 1}, \end{aligned} \quad (5)$$

hence, all the chaotic and nontrivial behavior disappears. Since most of the cellular automaton models [28] assume $A_- \rightarrow \infty$, we conclude that they are not able to describe the unpredictable behavior and complexities we are analyzing in this paper. Hence, the need to use the continuous models, with finite braking and accelerating capacities, to observe this complex and nontrivial behavior of the buses.

We find that both the light frequency ω and the bus-stop loading time γ can be used by planners to manipulate the bus travel time away from, or towards, regions of chaos. Increasing the bus-stop waiting time γ from zero, but keeping it nonstochastic, increases the travel time between lights, hence the bus motion resonates with the lights at a decreasing ω_1 while the complex dynamical regime is shifted to lower values of ω .

Figure 3 shows the effect of γ on the normalized average speed $\langle v \rangle / v_{\text{eff}}$ which is computed as follows. First, we start the bus from rest at the first traffic light and iterate the map through the next $N = 100$ traffic lights to eliminate the transient and reach the attractor. Then we take another $N = 100$ iterations of the map and calculate $\langle v \rangle / v_{\text{eff}} = N t_{\min} / t_N$ where t_N is the time taken to travel through the last N traffic lights, and $v_{\text{eff}} = v_c T_c / t_{\min}$ is the maximum average speed of the buses. A number of resonance peaks emerge, and we can deduce that

We calculate the Euclidean distance δ_n between the two trajectories and fit a Lyapunov exponent as

$$\delta_n = \delta_0 e^{\lambda n}. \quad (2)$$

This is repeated for ten initial conditions on the attractor and we report the Lyapunov exponent as the average of λ over these ten initial conditions. Of course, due to the nonsmooth nature of the map, we do not consider situations in which $\lambda \rightarrow \infty$. This is shown in Fig. 2(c), which clearly demonstrates that the dynamics is chaotic for the expected range of ω .

the maximum possible value at resonance is

$$\left. \frac{\langle v \rangle}{v_{\text{eff}}} \right|_{\max} = \frac{2A_+ A_- + (A_+ + A_-)}{2A_+ A_- (1 + \Gamma) + (A_+ + A_-)}. \quad (6)$$

Hence we have a synchronized state for a traffic light period $P \sim t_{\min}$ (namely at $\omega = \omega_1$) in the case of $\gamma = 0$.

We now consider what happens if the city planners cannot impose specific bus-stop loading time restrictions, i.e., γ at the n th bus stop becomes a stochastic variable dictated by instantaneous demand at that bus stop. For simplicity

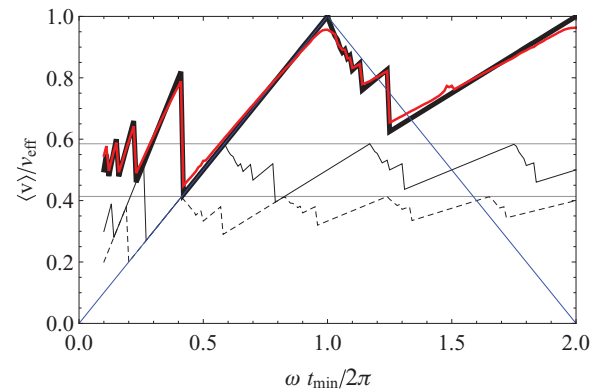


FIG. 3. (Color online) Average normalized speed $\langle v \rangle / v_{\text{eff}}$ as a function of the light's frequency for bus-stop loading times $\gamma = 0$ (thick line), $\gamma = T_c$ (thin line), and $\gamma = 2T_c$ (dashed line). After iterating the system to eliminate the transient and reach the attractor, we take another $N = 100$ iterations of the map and then calculate $\langle v \rangle / v_{\text{eff}} = N t_{\min} / t_N$ where t_N is the time taken to travel through N traffic lights. Peaks indicate light frequencies for which the bus never has to brake at traffic lights, i.e., the bus is synchronized with the green light. Horizontal lines correspond to Eq. (6). In red, we have included the behavior related to ten traffic lights, averaged over initial conditions with respect to the first traffic light. The predicted critical behavior near the resonance is shown in blue.

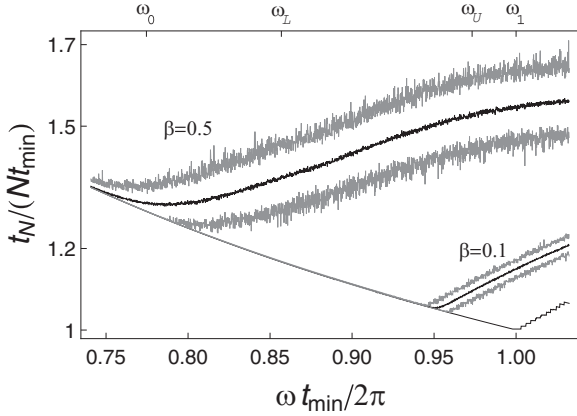


FIG. 4. Effect of stochastic bus-stop loading time γ (see text) on average travel time t_N/Nt_{\min} (black curves). Stochasticity parameter $\beta = 0, 0.1$, and 0.5 . Gray curves show minimum and maximum values for 100 different simulations using $N = 100$.

we choose $\gamma_n/T_c \in [0, \beta]$, $\beta > 0$, where γ_n is a uniformly distributed random number. Figure 4 shows the effect on the normalized average travel time between two successive traffic lights. The resonance frequency decreases as β increases, however, the average travel time increases, accompanied by an increase in its variability and hence unreliability of travel and arrival times. Given that we have used a uniform probability distribution for γ and that

$$\frac{1}{\beta T_c} \int_0^{\beta T_c} \frac{1}{\gamma + \zeta} d\gamma = \frac{1}{\beta} \ln \left(\frac{\zeta + \beta}{\zeta} \right), \quad (7)$$

we can approximate, from the expression for ω_1 in Eq. (4), the frequency at which we obtain the average minimum travel time for a given β . The result is

$$\frac{\bar{\omega}_1 T_c}{2\pi} \approx \frac{1}{\beta} \ln(1 + \beta T_c/t_{\min}). \quad (8)$$

In principle, we could also derive the analytical form for the standard deviation, but the result is not particularly illuminating.

Hence, we have shown that regimes of highly nontrivial dynamics (including chaos) lie close to the optimal solution in a simple one-body, one-dimensional system with periodic control lights and scheduled stops, even if loading times are negligible.

From Fig. 4 we can see that there are at least three effects that can be attributed to the stochastic waiting time. First, there is a shift in the resonance frequency to smaller values and an increase in the traveling time as expected from our previous discussion. Let us note that this combined effect is quite difficult to account for in advance since it requires having an estimation of the real time distribution of bus stop times, e.g., the number of passengers at each bus stop. This expected increase in the average traveling time is accompanied by an increase in its variability as $\langle \gamma \rangle$ increases, i.e., the introduction of a small degree of uncertainty in the bus-stop times is responsible for a high variability of traveling times near the resonance value. The last observation gives us some insight on strategies regarding the optimization of bus traveling

times. One could think that forcing the bus dynamics to synchronize with the traffic lights, assuming small bus-stop times, would tend to diminish, and thus optimize, the traveling times. However, here we have shown, with a very simple model under optimal conditions, that there is a nontrivial amount of traveling time unpredictability because the resonant behavior, in the case of minimal bus stopping time, is close to the region that displays nontrivial dynamics. Hence, having higher travel times and variability implies that any optimization scheme that relies on small stop times is destined to have high errors on the predicted traveling times due to the nontrivial behavior of this system close to resonance.

The observed increase in the variability of the travel time as we increase β can be explained in an intuitive manner. First, we note that for $\beta = 0$ the bus moving close to resonance on average will make it through many traffic lights before being forced to stop by a red light as it encounters almost the same green phase most of the time. For small β the velocity matching is not perfect so that the bus loses a small amount of the green phase at each traffic light. Eventually the bus exhausts the green phase and is required to stop, hence increasing the average number of times it is forced to stop at the traffic lights. This dynamics of exhausting the “green phase” occurs more often for larger β , hence increasing the variability.

These results provide certain suggestions for some realistic scenarios. First, although t_{\min} depends on L , v_{\max} , a_+ , and a_- , the values of L and v_{\max} are city dependent. We can observe from Fig. 3 (under the optimal situation with $\gamma_n = 0$) that $P = t_{\min} \sim 33$ s is the longest period for which we can have a synchronized state with a maximum average velocity. Of course, this estimation was done for $\gamma = 0$, therefore we should add to t_{\min} an expected passenger loading time $\langle \gamma \rangle$ so that we can synchronize the traffic lights with an effective period equal to the effective travel time between traffic lights, namely $P \sim t_{\min} + \langle \gamma \rangle$. Taking an average loading time of about 30 s, we reach an effective traffic light period of about a minute, which is similar to traffic light periods used in many cities. Furthermore, we note that for smaller v_{\max} or longer distances between traffic lights, the effective period may increase even more. Second, it is important to note that accounting for $\langle \gamma \rangle$ in the period is not enough, as Fig. 4 shows that fluctuations become relevant in the dynamics of the buses. Indeed, one of the most interesting results of our study is that we can see from Fig. 4 that the optimal frequency of the traffic lights depends on the distribution of the bus-stop waiting time γ , making it difficult to optimize the travel time of buses in cities *a priori*. Thus, this study may provide an explanation about the difficulty of optimizing the traveling time of buses in cities since the nontrivial and chaotic region, which is inherent in the bus behavior, lies close to the optimal resonant condition. Third, one may consider a sequence of traffic lights with an adaptive period, to account for variable loading time at each bus stop, a study that will be done elsewhere.

Even though there are many bus routes that have less bus stops than the number used to exhaust the transient in Figs. 2 and 3, characterizing the properties of the attractor as a function of ω provides intuition as to the inherent unpredictability of the bus system for ω below the resonance condition, even under the optimal situation of $\gamma_n = 0$. Furthermore, for the parameters in question, most of the effects of the transient behavior can

be disregarded in an average sense just after a few traffic lights (as few as ten), as shown by the red curve in Fig. 3 that displays the average velocity, averaged over an ensemble of initial conditions, after only ten traffic lights. This average is done by taking 100 buses that enter the road with a uniform distribution of initial time delays between zero and the period of the traffic light. We note that this curve is very similar to the corresponding $\gamma = 0$ curve (transient removed), with only very small deviations. Thus, we believe that the model may also be relevant for traffic situations with bus routes with just some tens of stops.

Some bus systems allow for a time slack that can be utilized by the bus drivers to control their schedule due to the passenger loading time unpredictability, however, this is done at the cost of increasing the travel time. Another possibility to reduce the unpredictability is to vary a_{\pm} and v_{\max} to adjust to a specific schedule. In this paper we have assumed the maximum values of a_{\pm} and v_{\max} , as restricted by speed limits and the acceleration capacity of the buses, therefore varying these parameters may reduce the unpredictability, but such a schedule would have a longer travel time.

In traffic systems we can expect the appearance of other stochastic and irregular elements, beyond the ones considered here, that would compound the above effects, increasing the unpredictability of the bus dynamics. If we include interacting buses in the system, we can introduce extra uncertainties in the bus behavior. For example, the authors of Ref. [29] showed that the passenger travel time of buses, using a different model, becomes unpredictable as two buses compete for passengers. Even though the variability introduced in the present paper is produced by the competition between two different time scales of a one-bus system, namely the traffic light timing and the stochastic loading passenger time, the introduction of interacting buses can increase the complexity of the passenger, or bus, travel times. We plan to analyze this situation elsewhere.

ACKNOWLEDGMENTS

This project was supported financially by FONDECYT under Contracts No. 1110135 (JAV), No. 1130273 (BAT), No. 1020391 (JR), No. 1030272 (JR), and No. 1121144 (VM). J. V. thanks COLCIENCIAS (Programa de Doctorados Nacionales) and CEIBA for their support.

APPENDIX

The map below completely determines the bus dynamics between consecutive traffic lights, given a set of initial conditions. For ease of description, we drop the n subscript and use the sequence of events described in Fig. 1, but we do not assume the bus starts standing still at a red light.

Region 1. The bus crosses the n th traffic light at position x_n , time t_n , with velocity v_n . It accelerates with a_+ until reaching velocity v_{\max} at position $x_{c1} = x_n + (v_{\max}^2 - v_n^2)/2a_+$, at time

$t_{c1} = t_n + (v_{\max} - v_n)/a_+$. Note that if $v_n = v_{\max}$ there is no need for this region.

Region 2. The bus moves at velocity v_{\max} until braking to fully stop at $x = x_n + l$. Braking must occur at the decision position $x_{s1} = x_n + l - v_{\max}^2/a_-$. The bus reaches the decision point at time $t_{s1} = t_{c1} + (x_{s1} - x_{c1})/v_{\max}$.

Region 3. The bus brakes with a_- . It reaches the bus stop at $x_n + l$ with speed 0, at time $t_l = t_{s1} + v_{\max}/a_-$.

Region 4. The bus loads and unloads passengers during a time γ .

Region 5. The bus accelerates with a_+ . So it is like region 1, but it now always starts from rest. At the end of the region, the bus is at position $x_{c2} = x_n + l + v_{\max}^2/2a_+$ with velocity $v_{c2} = v_{\max}$, at time $t_{c2} = t_l + \gamma + v_{\max}/a_+$.

Region 6. The bus moves at velocity v_{\max} until it reaches a second decision point, where it checks the status of the upcoming traffic light. If red, it has to be able to fully stop at $x = x_n + L$. As in region 2, the decision point is at $x_{s2} = x_n + L - v_{\max}^2/2a_-$, and it happens at time $t_{s2} = t_{c2} + (x_{s2} - x_{c2})/v_{\max}$. At this point, the bus has velocity $v_{s2} = v_{\max}$.

Region 7. The behavior depends on the light's status (i.e., red or green) at the decision time t_{s2} .

(A) If green, the bus does not brake. It reaches the next traffic light, which is at position $x_{n+1} = x_n + L$, with velocity $v_{n+1} = v_{\max}$ at time $t_{n+1} = t_{s2} + (v_{\max}^2/2a_-)/v_{\max} = t_{s2} + v_{\max}/2a_-$.

(B) If red, the bus starts braking. To decide what happens next, the time of the next green light must be calculated as follows:

$$t_g = \frac{2\pi}{\omega} \left(\left[\frac{\omega t_{s2} + \phi_n}{2\pi} \right] + 1 \right) - \frac{\phi_n}{\omega}, \quad (\text{A1})$$

where $[]$ represents the integer part. This time must now be compared to the time it will take the bus to fully stop $t_t = t_{s2} + v_{\max}/a_-$.

(a) If $t_t \leq t_g$, then the bus fully stops, and stays at the traffic light at position $x_{n+1} = x_n + L$, with velocity $v_{n+1} = 0$, until the next green light at $t_{n+1} = t_g$.

(b) If $t_t > t_g$ then the light turns green while the bus is braking (see region 8 in Fig. 1). This occurs at time t_g , at which the bus is at position $x_g = x_{s2} + v_{s2}(t_g - t_{s2}) - \frac{1}{2}a_-(t_g - t_{s2})^2$, with velocity $v_g = v_{s2} - a_-(t_g - t_{s2})$. Now the bus starts accelerating again. Again there are two cases. To decide, the position $x_c = x_{s2} + (v_{\max}^2 - v_g^2)/2a_+$ at which the bus reaches velocity v_{\max} , must be compared to the position of the next light, $x_n + L$.

(i) If $x_c < x_n + L$, the bus reaches maximum velocity before reaching the light. Thus it reaches the position x_c with velocity v_{\max} at time $t_c = t_g + (v_{\max} - v_g)/a_+$. Then it continues with velocity v_{\max} until reaching the light at position $x_{n+1} = x_n + L$ with velocity $v_{n+1} = v_{\max}$, at time $t_{n+1} = t_c + (x_n + L - x_c)/v_{\max}$.

(ii) If $x_c > x_n + L$, the bus reaches the next light at position $x_{n+1} = x_n + L$ with nonmaximum velocity $v_{n+1} = \sqrt{v_g^2 + 2a_+(x_n + L - x_g)}$, at time $t_{n+1} = (v_{n+1} - v_g)/a_+$.

[1] B. A. Toledo, E. Cerda, J. Rogan, V. Muñoz, C. Tenreiro, R. Zarama, and J. A. Valdivia, *Phys. Rev. E* **75**, 026108 (2007).

[2] L. A. Wastavino, B. A. Toledo, J. Rogan, R. Zarama, V. Muñoz, and J. A. Valdivia, *Physica A* **381**, 411 (2007).

- [3] T. Nagatani, *Rep. Prog. Phys.* **65**, 1331 (2002).
- [4] S. Lämmer and D. Helbing, *J. Stat. Mech.* (2008) P04019.
- [5] D. Helbing and M. Treiber, *Science* **282**, 2001 (1998).
- [6] B. A. Toledo, V. Muñoz, J. Rogan, C. Tenreiro, and J. A. Valdivia, *Phys. Rev. E* **70**, 016107 (2004).
- [7] B. Toledo, M. A. F. Sanjuan, V. Muñoz, J. Rogan, and J. A. Valdivia, *Commun. Nonlin. Sci. Num. Sim.* **18**, 81 (2013).
- [8] J. Villalobos, B. A. Toledo, D. Pastén, V. Muñoz, J. Rogan, R. Zarama, N. Lammoglia, and J. A. Valdivia, *Chaos* **20**, 013109 (2010).
- [9] S. Tadaki, M. Kikuchi, A. Nakayama, K. Nishinari, A. Shibata, Y. Sugiyama, and S. Yukawa, *J. Phys. Soc. Jpn.* **75**, 034002 (2006).
- [10] Y. Bar-Yam, *Unifying Themes in Complex Systems*, New England Complex Systems Institute Series on Complexity (Westview, Boulder, CO, 2003).
- [11] G. Nicolis and I. Prigogine, *Exploring Complexity: An Introduction* (W. H. Freeman and Company, New York, 1989).
- [12] A. Varas, M. D. Cornejo, B. A. Toledo, V. Muñoz, J. Rogan, R. Zarama, and J. A. Valdivia, *Phys. Rev. E* **80**, 056108 (2009).
- [13] C. Leduc, K. Padberg-Gehle, V. Varga, D. Helbing, S. Diez, and J. Howard, *Proc. Nat. Acad. Sci.* **109**, 6100 (2012).
- [14] O. H. Gao and R. A. Klein, *Transp. Res. D* **15**, 220 (2010).
- [15] H. Li and R. L. Bertini, *Transp. Res. Rec.* **2111**, 24 (2009).
- [16] J. X. Ding and H. J. Huang, *Acta Phys. Sin.* **59**, 3093 (2010).
- [17] C. Q. Mei, H. J. Huang, T. Q. Tang, and H. W. Wang, *Acta Phys. Sin.* **58**, 1497 (2009).
- [18] C.-F. Liao and G. A. Davis, *Transp. Res. Rec.* **2034**, 82 (2007).
- [19] N. B. Hounsell, B. P. Shrestha, F. N. McLeod, S. Palmer, T. Bowen, and J. R. Head, *IET Intell. Transp. Sys.* **1**, 131 (2007).
- [20] S.-G. Li and Y.-F. Ju, *IEEE Trans. Intell. Transp. Sys.* **10**, 236 (2009).
- [21] K. Sakamoto, C. Abhayantha, and H. Kubota, *Transp. Res. Rec.* **2034**, 103 (2007).
- [22] V. Arasan and P. Vedagiri, *J. Infrastruct. Syst.* **15**, 305 (2009).
- [23] A. Cain, G. Darido, M. R. Baltes, P. Rodriguez, and J. C. Barrios, *Transp. Res. Rec.* **2034**, 45 (2007).
- [24] A. Gilbert, *Transp. Rev.* **28**, 439 (2008).
- [25] D. A. Hensher and T. F. Golob, *Transportation* **35**, 501 (2008).
- [26] L. A. Koehler and W. Kraus, Jr., *Transp. Res. C* **18**, 288 (2010).
- [27] C. Gershenson and L. A. Pineda, *PLoS ONE* **4**, e7292 (2009).
- [28] K. Nagel and M. Schreckenberg, *J. Physique I* **2**, 2221 (1992).
- [29] T. Nagatani, *Phys. Rev. E* **68**, 036107 (2003).